

I.T. Christodoulou, V.E. Alexopoulou, N.E. Karkalos,  
E.L. Papazoglou, A.P. Markopoulos, Athens, Greece

## **ON THE SURFACE ROUGHNESS OF 3D PRINTED PARTS WITH FDM BY A LOW-BUDGET COMMERCIAL PRINTER**

**Abstract.** *As additive manufacturing machines price is decreasing, while, at the same time, the expertise in the relevant field is rising, it is essential to test and evaluate the low-budget machines that are available for commercial use. Whilst low-budget machines are widely utilized for rapid prototyping and experimentation, they are not capable of producing parts with high surface quality and achieve high levels of repeatability due to low quality hardware and not optimized software. Having said that, the main aim of the current study is to experiment with a low budget Fused Deposition Modeling (FDM) 3D-Printer, and evaluate the surface roughness of the printed parts in respect to the angle from the print plate. Polylactic Acid (PLA) was chosen as filament material, while the printed parts surface roughness was measured according to the ISO ASTM 52902-2021 standard. The surface roughness was estimated in terms of the  $R_a$  and  $R_z$  values, while a statistical analysis was implemented in order some interesting conclusions to be deduced regarding the correlation between part orientation and surface quality.*

**Keywords:** *additive manufacturing machines; rapid prototyping; Fused Deposition Modeling; surface roughness; 3D-Printer.*

### **Introduction**

Over the last decades, Additive Manufacturing (AM) processes have become a hot topic for both the researching and the industrial world, as they can give highly customized and geometrically complex products. In AM, a 3D-CAD model is virtually broken down into 2D-cross sections and the final product is built by consecutive layers [1]. Many AM techniques have been developed, such as vat polymerization (SLA), powder bed fusion (SLS, SLM) and material extrusion (FDM).

Specifically, in Fused Deposition Modeling (FDM), a thermoplastic filament (such as PLA, ABS, PEEK, etc.), which is stored in a reservoir, is heated up to the melting temperature and then it is extruded through a nozzle tip on the 3d-printing bed [2]. Several parameters affect the characteristics and the quality of the building part. Some of them are the build orientation, the layer height, the raster angle, the air gap, the printing speed, the infill density, the infill pattern, the extrusion temperature and the nozzle diameter [3].

Most of the published papers study the impact of these parameters on the mechanical properties of the final products. Es-Said et al.[4] carried out experiments with FDM-produced ABS samples with 0°, 45° and 90° raster angle. The results showed that the highest ultimate, yield and bending strength are

reached for  $0^\circ$ , whereas  $45^\circ$  and  $90^\circ$  are much weaker orientations and may lead to delamination of the layers. Ashtankar et al. [5] tested FDM-processed ABS samples in five different orientations ( $0^\circ$ ,  $30^\circ$ ,  $45^\circ$ ,  $60^\circ$ ,  $90^\circ$ ) and concluded that both maximum tensile and compressive strength reduce as the build orientation varies from  $0^\circ$  to  $90^\circ$ . Baich et al. [6] investigated the effect of infill density on the tensile, compressive and bending strength of FDM-manufactured ABS specimens. Specifically, three different infill densities were tested and compared with solid ABS specimens: low density, high density and double density. In compression and bending tests the results showed that double dense samples achieved higher properties, as expected. On the other hand, the result of the tensile test was counter-intuitive, as the high dense sample achieved higher strength compared to the double dense sample. De Toro et al. [7] investigated the impact of layer height, printing pattern, infill density and nozzle diameter on the tensile and bending behavior of FDM-printed CRF-Nylon parts. The results showed that infill density is the most crucial parameter in order to achieve good tensile and bending behaviors. Moreover, lower layer heights result in better bending properties, whereas the printing pattern influences more the tensile behavior of the component. On the other hand, nozzle diameter had not a significant influence on the tensile and bending properties. As follows from the analysis of this paragraph, a great number of experiments have been done in order to study the impact of the different FDM parameters on the mechanical properties of the final products. However, in Mechanical Engineering, strength is not the only property that judges the quality of a product. For this reason, tests should not only be limited on mechanical properties, but they should also take into consideration the surface roughness of the products, as well.

Although, surface roughness is a crucial factor when studying FDM processes, yet the experimental work that has been carried out is limited. Lin et al. [8] processed with FDM methods the following three materials: 1% alginate/7% gelatin hydrogel, 3% alginate/7% gelatin hydrogel and poloxamer paste. The results showed that conical nozzles, high pressures and large nozzle-to-platform gap generally reduce the surface roughness. However, there is a need for calibration of these three parameters for each material. Moreover, a slight limitation of this study is the fact that extrusion stress caused by these parameters is not taken into consideration. Sandhu et al. [9] carried out experiments with FDM-processed PLA samples. Specifically, they tested the impact of layer thickness (0.16mm, 0.2mm, 0.28mm), raster angle ( $30^\circ$ ,  $45^\circ$ ,  $60^\circ$ ) and infill pattern (octet, quarter-cubic, cubic) on the surface roughness of the samples, along  $X$  and  $Y$  axis. They concluded that the surface roughness in both  $X$  and  $Y$  axis lies in, approximately, the same range and the best result is given for the combination of 0.16mm layer thickness,  $60^\circ$  raster angle and cubic infill pattern.

Several researchers have studied the impact of build orientation on the surface roughness. Koziar et al. [10] pointed out the significant impact of build orientation on the surface roughness of SLM-processed 316L Stainless Steel parts. However, these observations should be ratified and for other material, such as thermoplastics in order to achieve a more general view of the build orientation-surface roughness correlation. Buj-Corral et al. [11] and Alsoufi et al. [12] carried out some very interesting experiments in order to find out the build orientation-surface roughness correlation in FDM-printed PLA parts. However, both their studies are based on case-sensitive (cylindrical FDM-processed samples) and the measurements are not according to a standard regulation, so their results cannot be generalized. For this reason, there is a need to carry out experiments, with the strict specifications that the ISO standards recommend. By following these regulations, the experiments will be much more consistent, which will be very valuable when it comes to understanding and simulating these phenomena.

The target of this paper is to calculate the build orientation-surface roughness correlation of FDM-printed PLA samples, according to ISO ASTM 52902-2021. The novelty of this paper is the use of a low-cost FDM-printer in order to ascertain whether low-budget 3D-printers can give parts with acceptable (according to ISO ASTM 52902-2021) surface roughness.

### **Materials and Methods**

The material used in this paper is PLA with its properties listed in the Table 1, while the utilized

Table 1 – PLA properties and technical specifications

<b>PLA Properties – specifications</b>	
Manufacturer	Real Filament
Manufacturer's preferred hot-end temperature	205 °C
Manufacturers preferred heating bed temperature	40 °C
Specific gravity	1.24 g/cc
Tensile strength	16 kpsi (machine direction, MD) / 21 kpsi (traverse direction, TD)
Elongation at break	160% (MD) 100% (TD)
Tensile modulus	480 MPa (MD) 560 MPa (TD)
Impact strength	2.5 J
Melt temperature	210 °C +/- 8 °C
Melting point	145-160 °C

Vicat softening temperature	60 °C
-----------------------------	-------



Figure 1 – PLA Filament that was utilized

The low-budget 3D-Printer used in this case is the Ender 3 with direct drive extruder set up, whilst the Cura 4.12 was chosen as the slicer software. The basic settings that been utilized are presented in the Table 2, while the full detailed list of Cura Software Settings can be provided and will be in CSV format.

Table 2 – 3D printing main parameters

<b>3D Printing main parameters</b>	
Layer Height	0.16 mm
Wall Line Count	4
Infill Density	45.0%
Printing Temperature	205
Build Plate Temperature	67
Print Speed	50 mm/s
Retraction	Enabled
Fan Speed	75%
Build Plate Adhesion Type	Brim

In Figures 2 and 3 the Cura GUI environment is depicted, as well as the respective roughness test prints.

The measurements were taken on both sides of the test prints, with these sides were named “UP” and “DOWN” respectively. For the surface roughness measurements, a Taylor Hobson Surtronic 3+ profilometer was employed (see

Figure 4). Based on the ISO ASTM 52902-2021, on each specimen side three roughness measurements were taken at different locations, in a direction perpendicular to the lay pf the texture (i.e., along the samples' length). The evaluation length was set 12.5 mm and the sampling length ( $\lambda_C$ ) at 2.5 mm.

The suggested number of samples for this test is five according to the AS ISO ASTM 52902-2021. The measured values are the arithmetical mean deviation of the assessed profile known as Ra and the average distance between the highest peak and lowest valley in each sampling length known as Rz, which are calculated by the equations shown below [13,14]:

$$R_a = \frac{1}{l_r} \int_0^{l_r} |z(x)| dx \quad (1)$$

where  $l_r$  is the length where measurements are taken,  $X$  is the length axis, and  $Z$  is the height from valleys to peaks.

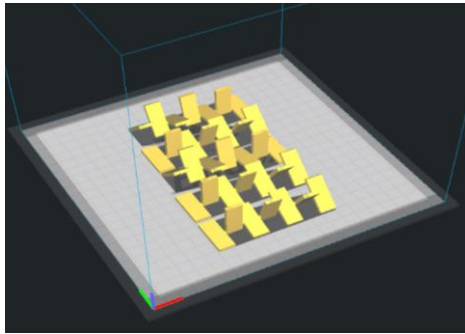


Figure 2 – Cura GUI Environment, Settings, and the part arrangement on the build plate of the 3D-Printer are visible

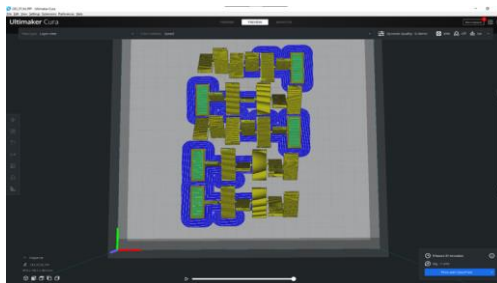


Figure 3 – Printing lines orientations are perpendicular to the long side of the parallelogram with  $0^\circ$  angle from the bed



Figure 4 – Taylor Hobson Surtronic 3+

$$R_z = \frac{1}{s} \sum_{i=1}^s R_{t_i} \quad (2)$$

where  $s$  is the number of sampling lengths and  $R_{t_i}$  is  $R_t$  of the  $i$ th sample. The assessment of the surface roughness is done based on the mean values of  $R_a$  and  $R_z$  for each angle, and the respective coefficient of variation as well. The coefficient of variation considers the mean value and the standard deviation, and is calculated by eq. 3 [14]:

$$c_v = \frac{\sigma}{\mu} \quad (3)$$

where  $\sigma$  is the standard deviation and  $\mu$  the average of the sample.

### **Results and Discussion**

The parts geometry and the obtained prints based on the AS ISO ASTM 52902-2021 is presented in Figure 5.



Figure 5 – 3D-Printed parts

In Tables 3 – 6 the surface measurements of  $R_a$  and  $R_z$  are listed along with the respective mean values, standard deviations, and the coefficients of variation.

Table 3 –  $R_a$  measurements for the Up surface

<b><math>R_a</math> – Up Surface</b>								
# of spec.	# of meas.	0°	15°	30°	45°	60°	75°	90°
1	1	0.00	15.00	30.00	45.00	60.00	75.00	90.00
	2	13.80	32.20	26.00	26.80	24.80	20.80	14.20
	3	11.60	31.60	25.80	26.20	22.60	16.40	15.40
2	1	12.20	33.20	28.40	26.20	25.60	18.00	15.00
	2	18.60	33.40	27.60	25.80	27.40	19.60	19.80
	3	19.00	35.20	27.80	25.80	26.20	20.80	19.60
3	1	19.80	35.20	27.40	24.80	30.80	22.00	19.00
	2	14.00	37.80	30.60	23.60	31.60	x	15.20
	3	15.80	36.60	29.00	23.60	23.20	x	15.00
4	1	14.60	43.20	33.00	23.80	21.60	x	14.00
	2	17.00	9.20	25.60	22.80	21.60	20.00	18.40
	3	16.60	9.20	25.80	23.40	19.00	18.40	18.60
5	1	17.20	9.00	25.40	22.60	20.20	23.00	17.20
	2	7.80	38.80	27.40	25.00	22.40	22.60	18.60
	3	7.80	36.80	26.40	24.80	21.20	21.00	19.40
Mean value in $\mu\text{m}$			8.80	38.40	26.00	25.40	21.40	20.40
Standard deviation in $\mu\text{m}$			14.31	30.65	27.48	24.71	23.97	20.25
Coefficients of variation			3.97	11.51	2.11	1.33	3.73	1.93

Table 4 –  $R_z$  measurements for the Up surface

<b><math>R_z</math> – Up Surface</b>								
# of spec.	# of meas.	0°	15°	30°	45°	60°	75°	90°
1	1	85.00	168.00	139.00	156.00	144.00	132.00	81.00
	2	80.00	169.00	137.00	160.00	133.00	97.00	91.00
	3	86.00	168.00	161.00	160.00	156.00	110.00	85.00
2	1	105.00	164.00	156.00	146.00	153.00	122.00	129.00
	2	112.00	175.00	168.00	144.00	151.00	124.00	123.00
	3	124.00	174.00	164.00	139.00	181.00	133.00	106.00
3	1	91.00	181.00	166.00	139.00	195.00	x	93.00
	2	99.00	178.00	153.00	136.00	133.00	x	94.00
	3	96.00	220.00	174.00	135.00	133.00	x	82.00
4	1	117.00	51.00	132.00	129.00	122.00	116.00	109.00

5	2	119.00	54.00	130.00	136.00	113.00	108.00	110.00
	3	117.00	45.00	131.00	128.00	116.00	145.00	96.00
	1	55.00	211.00	142.00	142.00	132.00	132.00	111.00
	2	62.00	197.00	140.00	134.00	125.00	119.00	126.00
	3	60.00	205.00	140.00	143.00	135.00	118.00	106.00
Mean value in $\mu\text{m}$			93.87	157.33	148.87	141.80	141.47	121.33
Standard deviation in $\mu\text{m}$			22.53	58.09	14.97	10.12	22.88	13.05
Coefficients of variation			0.24	0.37	0.10	0.07	0.16	0.11

Table 5 –  $R_a$  measurements for the Down surface

<b><math>R_a</math> – Down Surface</b>								
# of spec.	# of meas.	0°	15°	30°	45°	60°	75°	90°
1	1	x	x	x	15.60	18.20	18.20	14.60
	2	x	x	x	15.40	14.80	17.80	17.20
	3	x	x	x	15.60	16.00	19.40	13.60
2	1	x	x	x	15.60	16.80	19.40	16.40
	2	x	x	x	16.40	19.00	17.80	15.40
	3	x	x	x	17.80	17.80	18.40	14.20
3	1	x	x	x	16.20	16.00	13.40	14.00
	2	x	x	x	18.40	15.80	14.00	14.40
	3	x	x	x	20.80	20.20	14.20	13.60
4	1	x	x	x	14.60	3.60	18.80	16.80
	2	x	x	x	14.60	7.40	17.40	15.00
	3	x	x	x	15.40	5.60	19.80	14.20
5	1	x	x	x	20.40	x	18.00	16.00
	2	x	x	x	20.20	x	21.80	17.40
	3	x	x	x	21.00	x	18.40	16.20
Mean value in $\mu\text{m}$			-	-	-	17.20	14.27	17.79
Standard deviation in $\mu\text{m}$			-	-	-	2.36	5.53	2.30
Coefficients of variation			-	-	-	0.14	0.39	0.13

Table 6 –  $R_z$  measurements for the Down surface

<b><math>R_z</math> – Down Surface</b>								
# of spec.	# of meas.	0°	15°	30°	45°	60°	75°	90°
1	1	x	x	x	90.00	106.00	114.00	84.00
	2	x	x	x	89.00	94.00	115.00	94.00
	3	x	x	x	92.00	101.00	124.00	99.00
2	1	x	x	x	86.00	97.00	113.00	97.00

	2	x	x	x	97.00	108.00	104.00	91.00
	3	x	x	x	105.00	101.00	100.00	87.00
3	1	x	x	x	99.00	88.00	75.00	85.00
	2	x	x	x	107.00	96.00	75.00	94.00
	3	x	x	x	118.00	124.00	85.00	84.00
4	1	x	x	x	82.00	25.00	114.00	106.00
	2	x	x	x	80.00	40.00	100.00	86.00
	3	x	x	x	89.00	23.00	120.00	83.00
5	1	x	x	x	120.00	x	103.00	103.00
	2	x	x	x	114.00	x	132.00	111.00
	3	x	x	x	126.00	x	100.00	108.00
Mean value in $\mu\text{m}$			-	-	-	99.60	83.58	104.93
Standard deviation in $\mu\text{m}$			-	-	-	14.65	34.12	16.74
Coefficients of variation			-	-	-	0.15	0.41	0.16

Based on the experimental data of Tables 3 – 6, the charts for  $R_a$  and  $R_z$  depending on the angle to the build plate can be drawn, which are presented in Figures 6 and 7.

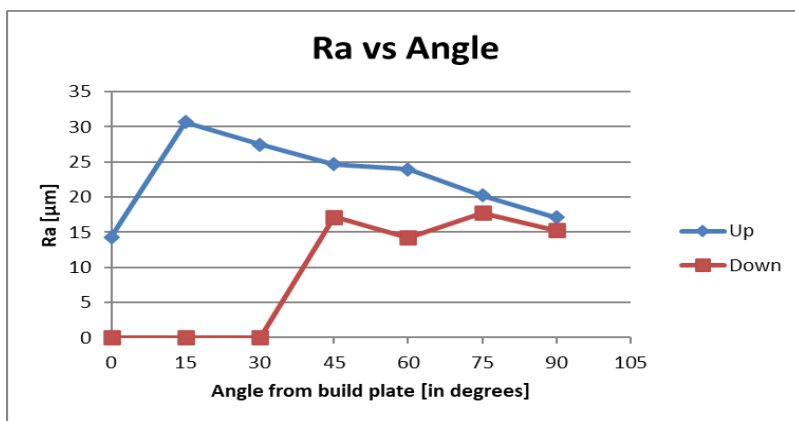


Figure 6 –  $R_a$  to Angle Degrees from build plate

Based on the charts of Figure 5, it can be deduced that mean  $R_a$  values on the up side are low for the 0° angle, then they increased up to 30.65  $\mu\text{m}$  for the 15°, and finally they descend to 17.09 for the 90°. The mean  $R_a$  for the Down surface has a more vague behavior, since it has only a small variation depending on the angle, while, this deviation is not monotonous. Another interesting observation

regarding the correlation between the surface roughness of the Up and Down side of the printed part can be also deduced. The values are getting more similar as the printed part orientation changes to be perpendicular to the build surface, where the roughness of each side should be equal. Unfortunately, due to measurement errors, 3D-printer accuracy and other parameters, the measurements cannot be exactly similar for the 90°. Moreover, it is visible that the Up side of the parts are rougher than the other Down side for all the angles.

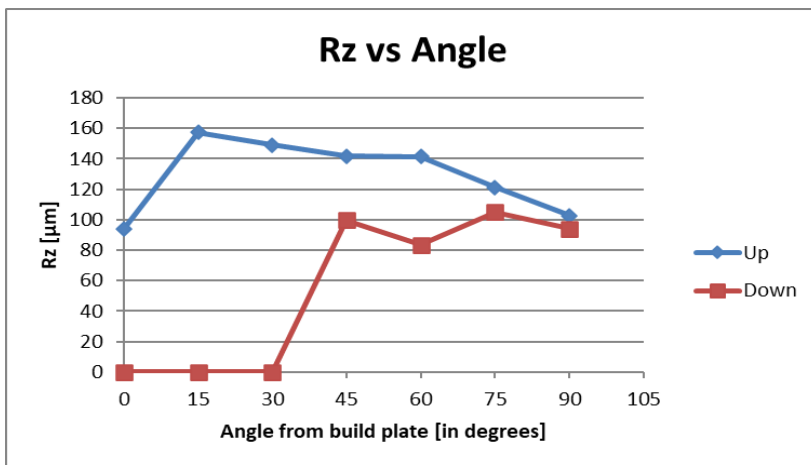


Figure 7 –  $R_z$  to Angle Degrees from build plate

Regarding the  $R_z$  values, and based on the diagrams of Figure 6, it is visible that the mean  $R_z$  values follow the same trend as the  $R_a$ . For the up side, at first, mean  $R_z$  is as low as 93.86 µm, then it peaks to 157.33 µm at 15 degrees and it is gradually descending to 102.8 µm for the 90°. For the down side, again the samples for 0, 15 and 30 degrees could not be measured due to overrange values at 15 and 30 degrees, or because (for the 0°) the surface was in touch with the building plate. Other than that, the downside has smaller values for the 45, 60 and 75 degrees and at 90 degrees the values of  $R_z$  are very close, almost similar. It can be said that non measurable values for 15 and 30 degrees at the Down side has been created due to lack of sufficient cooling and inaccuracy of the printer. The same conclusion can be reasonably deduced for the high  $R_z$  values at 15° on the up side of the parts.

Finally, by the plots for the coefficient of variation of Figure 8, it is possible to get to some interesting conclusions regarding the repeatability. The 45 degrees

have significantly low coefficient of variation, meaning that the surface finish was very similar in all the samples and in both surfaces (i.e., Up and Down). A big difference between the coefficient is visible on the Up side of the part and the Down side of the part for the 60°. This is due to reasons such as lack of structural supports and not sufficient and proper cooling. In all the samples the worst scenario is the samples that were printed in 15 degrees from the build plate, which also have a very high coefficient of variation. This is expected reasonable since, for the 15° the unsupported surface is even bigger, and the not fully cooled material is pulled by the gravity, creating a rough and nonuniform surface.

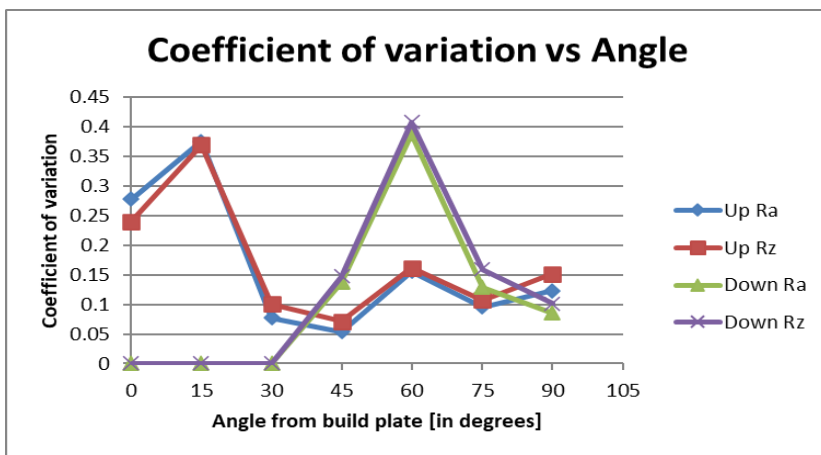


Figure 8 – Coefficient of variation vs Angle degrees from build plate for the  $R_a$  and  $R_z$  for the Up and Down surfaces

Last but not least, it is visible that even though 30 and 45 degrees have the smallest coefficient of variation, meaning that in these angles the produced parts will have similar surface roughness, they do not have the smallest  $R_a$  or  $R_z$  values. This is a trade-off the user of such a machine must accept as he can choose to reliably create parts of bigger surface roughness or create parts with smaller surface roughness unreliably.

### Conclusions

In the current study, an experimental investigation of surface roughness in 3D printed parts manufactured by a low budget 3D-print machine was studied. The creation of the 3D-printed parts was performed according to ISO AS ISO ASTM

52902-2021, as well all the measurements. For each angle, 5 specimens were built and the surface roughness was measured on the Up and Down surface. The assessment of the surface roughness was made based on the  $R_a$  and  $R_z$  mean values, as well the respective coefficient of variation. The main deduced conclusions are:

- A low budget machine cannot produce parts with low  $R_a$  and  $R_z$  values reliably.
- A trade-off should be conducted between reliably producing parts with big  $R_a$  and  $R_z$  values or unreliably and unrepeatably producing parts with small  $R_a$  and  $R_z$  values.
- This machine due to lack of cooling, lack of second extruder for water soluble support and not so high quality of the hardware, as well as not optimized software and firmware, cannot produce reliably parts with good surface roughness on both sides, i.e., Up and Down.

**References:** 1. A. Rashid, "Additive Manufacturing Technologies," *CIRP Encycl. Prod. Eng.*, pp. 1–9, 2019, doi: 10.1007/978-3-642-35950-7\_16866-1. 2. S. Vyavahare, S. Teraiya, D. Panghal, and S. Kumar, "Fused deposition modelling: a review," *Rapid Prototyp. J.*, vol. 26, no. 1, pp. 176–201, 2020, doi: 10.1108/RPJ-04-2019-0106. 3. I. J. Solomon, P. Sevel, and J. Gunasekaran, "A review on the various processing parameters in FDM," *Mater. Today Proc.*, vol. 37, no. Part 2, pp. 509–514, 2020, doi: 10.1016/j.matpr.2020.05.484. 4. O. S. Es-Said, J. Foyos, R. Noorani, M. Mendelson, R. Marloth, and B. A. Pregger, "Effect of layer orientation on mechanical properties of rapid prototyped samples," *Mater. Manuf. Process.*, vol. 15, no. 1, pp. 107–122, 2000, doi: 10.1080/10426910008912976. 5. K. M. Ashtankar, A. M. Kuthe, and B. S. Rathour, "IMECE2013-63146," pp. 1–7, 2016. 6. L. Baich, G. Manogharan, and H. Marie, "Study of infill print design on production cost-time of 3D printed ABS parts," *Int. J. Rapid Manuf.*, vol. 5, no. 3/4, p. 308, 2015, doi: 10.1504/ijrapidm.2015.074809. 7. E. V. De Toro, J. C. Sobrino, A. M. Martínez, and V. M. Eguía, "Analysis of the influence of the variables of the fused deposition modeling (FDM) process on the mechanical properties of a carbon fiber-reinforced polyamide," *Procedia Manuf.*, vol. 41, pp. 731–738, 2019, doi: 10.1016/j.promfg.2019.09.064. 8. Z. Lin, T. Jiang, J. M. Kinsella, J. Shang, and Z. Luo, "Assessing roughness of extrusion printed soft materials using a semi-quantitative method," *Mater. Lett.*, vol. 303, no. July, p. 130480, 2021, doi: 10.1016/j.matlet.2021.130480. 9. G. S. Sandhu, K. S. Boparai, and K. S. Sandhu, "Effect of slicing parameters on surface roughness of fused deposition modeling prints," *Mater. Today Proc.*, no. xxxx, 2021, doi: 10.1016/j.matpr.2021.09.047. 10. T. Kozior and J. Bochnia, "The influence of printing orientation on surface texture parameters in powder bed fusion technology with 316L steel," *Micromachines*, vol. 11, no. 7, 2020, doi: 10.3390/M11070639. 11. I. Buj-Corral, A. Domínguez-Fernández, and R. Durán-Llucà, "Influence of print orientation on surface roughness in fused deposition modeling (FDM) processes," *Materials (Basel)*, vol. 12, no. 23, 2019, doi: 10.3390/ma12233834. 12. M. S. Alsoufi, A. El-Sayed, and A. E. Elsayed, "How Surface Roughness Performance of Printed Parts Manufactured by Desktop FDM 3D Printer with PLA+ is Influenced by Measuring Direction," *Am. J. Mech. Eng.*, vol. 5, no. 5, pp. 211–222, 2017, doi: 10.12691/ajme-5-5-4. 13. Whitehouse, David (2012). *Surfaces and their Measurement*. Boston: Butterworth-Heinemann. ISBN 978-0080972015. 14. Everitt, Brian (1998). *The Cambridge Dictionary of Statistics*. Cambridge, UK New York: Cambridge University Press. ISBN 978-0521593465.

Іоаніс Т. Христодулу, Василикі Е. Алексопулу, Ніколаос Е. Каркалос,  
Емануїл Л. Папазоглу, Ангелос П. Маркопулос, Афіни, Греція

## **ПРО ШОРСТКІСТЬ ПОВЕРХНІ ДЕТАЛЕЙ ДРУКОВАНИХ ЗА ТЕХНОЛОГІЄЮ FDM З ВИКОРИСТАННЯМ МАЛОБЮДЖЕТНОГО КОМЕРЦІЙНОГО 3D ПРИНТЕРА**

**Анотація:** *Оскільки ціни на машини для адитивного виробництва знижуються, а досвід у відповідній галузі зростає, важливо тестувати та оцінювати малобюджетні машини, доступні для комерційного використання. Хоча малобюджетні верстати широко використовуються для швидкого прототипування та експериментів, вони не здатні виробляти деталі з високою якістю поверхні та досягати високого рівня повторюваності із-за низькоякісного обладнання та неоптимізованого програмного забезпечення. При цьому основною метою поточного дослідження є проведення експериментів з малобюджетним 3D-принтером для моделювання методом наплавлення (FDM) та оцінка шорсткості поверхні надрукованих деталей в залежності від кута відносно друкуючої форми. В якості філаментного матеріалу була обрана полімолочна кислота (PLA), а шорсткість поверхні друкуючих деталей вимірювалася відповідно до стандарту ISO ASTM 52902-2021. Шорсткість поверхні оцінювалася з огляду значень  $R_a$  і  $R_z$ , а також був проведений статистичний аналіз, щоб зробити деякі цікаві висновки щодо кореляції між орієнтацією деталі та якістю поверхні. Для кожного кута виготовляли по 5 зразків та вимірювали шорсткість поверхні на верхній та нижній поверхнях. Оцінку шорсткості поверхні проводили за середніми значеннями  $R_a$  і  $R_z$ , а також відповідним коефіцієнтом варіації. Основними висновками є такі: малобюджетний верстат не може надійно виробляти деталі з низькими значеннями  $R_a$  та  $R_z$ ; необхідно знайти компроміс між надійним виробництвом деталей з великими значеннями  $R_a$  та  $R_z$  або ненадійним та неповторним виробництвом деталей з малими значеннями  $R_a$  та  $R_z$ ; дана машина через відсутність охолодження, відсутність другого екструдера для водорозчинної підкладки і не настільки високої якості апаратної частини, а також не оптимізованого програмного забезпечення та прошивки, не може надійно виробляти деталі з гарною шорсткістю поверхні з обох боків, тобто зверху та знизу.*

**Ключові слова:** *машини для адитивного виробництва; швидке створення прототипів; моделювання плавного осадження; шорсткість поверхні; 3D-принтер.*